Supplementary Materials

S1. Adsorption Isotherms

The pure component adsorption isotherms of O_2 and N_2 on zeolite (OX-19, CECA, France) were measured using the static volume method. The pressure range was 0–3 bar at 253 K, 273 K, and 298 K, and the measuring apparatus was BSD-PH (Beishide Instrument Technology, Beijing, instrument repeatability error within 2 % and the pressure sensor accuracy is 0.01% F.S). The zeolite was activated before the measurement at a temperature of 300 °C for 120 min. The pressure was raised by about 0.05 bar per time and equilibrated for 3600 s, and the purity for O_2 and N_2 was 99.999% (Beiwen Gas Manufacturing Factory, Beijing). The experiment was repeated three times to reduce the operating and random errors.

The adsorption isotherms are shown in Figure S1. At the same temperature, the adsorption of N_2 was significantly higher than that of O_2. As the temperature decreased, the adsorption amount of both N_2 and O_2 increased significantly. Based on this result, the fitted IP_{1-4} was required in the Extended Langmuir 2 equation. The fitting results are as Figure S2 and Table S2 show.

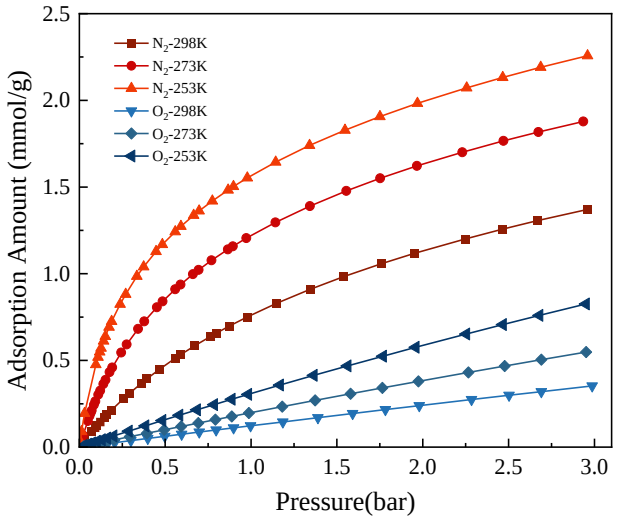

Figure S1. Adsorption isotherms for nitrogen and oxygen.

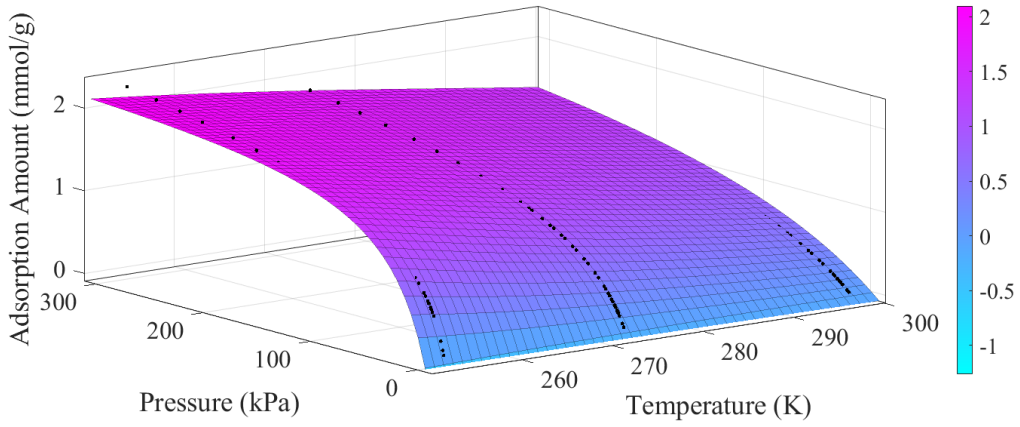

(**a**)

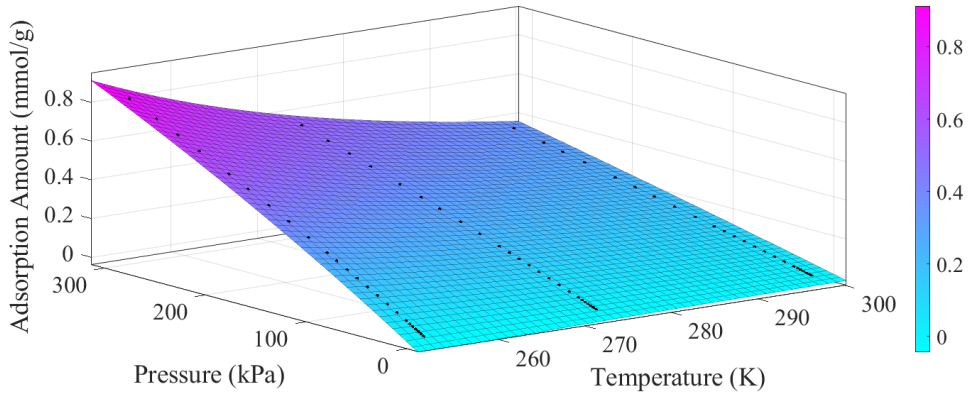

(**b**)

Figure S2. (**a**) Adsorption amount of N_2 at different pressures and temperatures; (**b**) adsorption amount of O_2 at different pressures and temperatures.

Table S1. Adsorption isotherm parameter fitting results.

Parameters	N_2	95% CI	O_2	95% CI
IP_1 (mol·kg^{-1}·kPa^{-1})	2.756×10^{-6}	(1.245×10^{-6}, 4.267×10^{-6})	6.025×10^{-6}	(5.75×10^{-6}, 6.301×10^{-6})
IP_2 (K)	2494	(2348, 2641)	1593	(1581,1605)
IP_3 (kPa^{-1})	1.391×10^{-6}	(4.739×10^{-8}, 2.735×10^{-6})	1.487×10^{-6}	(4.632×10^{-7},2.51×10^{-6})
IP_4 (K)	2449	(2195, 2703)	1503	(1326, 1679)
R^2	0.9939	/	0.9999	/
SSE	0.2131	/	7.744×10^{-5}	/
RMSE	0.04687	/	0.001067	/

S2. Fix Bed Breakthrough

Multi-component adsorption experiments were carried out on a fixed bed device. The experiments used the multi-component adsorption breakthrough curve analyzer (BSD-MAB, Beishide instrument technology, Beijing). Before the start of the experiment, the zeolite was flushed using He at 573 K for 120 min; the test temperature was 298 K, the volumetric percentage concentration of the components was 78% for N_2 and 22% for O_2, the total flowrate was 10 sccm, and the purity for O_2 and N_2 was 99.999% (Beiwen Gas Manufacturing Factory, Beijing).

The experimental breakthrough curve is shown in Figure S2. N_2 was preferentially adsorbed, O_2 was gradually detected, and the volumetric concentration percent was maintained above 90% for some time, meeting the demand for oxygen production.

The breakthrough curve was simulated and compared with the experimental breakthrough curve. The result is shown in Figure S3. This validated the reliability of the relevant parameters of the adsorption bed. The model diagram is shown in Figure S4, where feed is the inlet module, bed is the adsorption bed, and product is the outlet module.

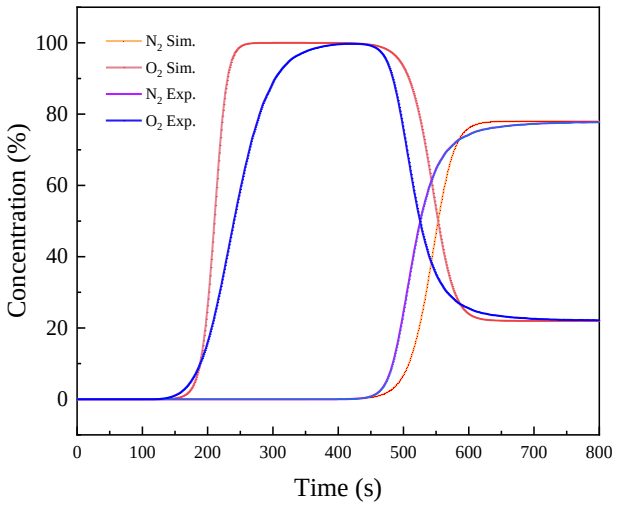

Figure S3. Experimental and simulated breakthrough results.

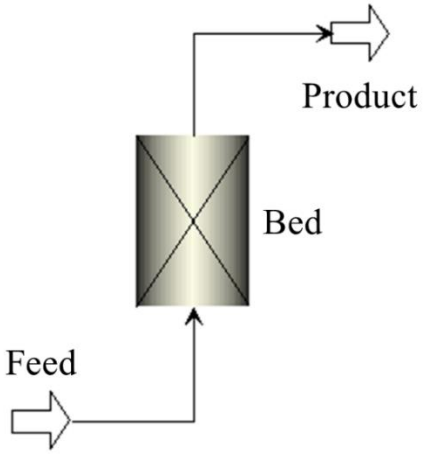

Figure S4. Breakthrough model in Aspen Adsorption.

S3. Results of Plateau Optimization Simulation

The feed flowrate and product flowrate were changed to simulate the feed flowrate of 160 m^3/h, 180 m^3/h, 200 m^3/h, 220 m^3/h and 240 m^3/h at altitudes of 3000 m, 4000 m and 5000 m, with the Cv from 1.2 mol/s/MPa to 1.5 mol/s/MPa. The results are presented in Tables S2–S4 below.

Table S2. Simulation results of different feed flow rate and Cv at 3000 m.

No.	Cv mol/s/MPa	Feed Flowrate m^3/h	Pro. m^3/h	En. MJ/m^3	Pur. %	Rec. %
1	1.2	160	2.73	1.37	91.54	19.37
2	1.2	180	3.13	1.35	91.52	20.59
3	1.2	200	3.52	1.35	91.44	21.69
4	1.2	220	3.91	1.35	91.48	22.67
5	1.2	240	4.30	1.36	91.55	23.53
6	1.3	160	2.88	1.30	91.22	19.37
7	1.3	180	3.29	1.28	91.15	20.59
8	1.3	200	3.70	1.28	91.11	21.69
9	1.3	220	4.11	1.28	91.10	22.67
10	1.3	240	4.53	1.29	91.08	23.53
11	1.4	160	3.00	1.24	90.85	20.10

12	1.4	180	3.44	1.22	90.75	21.45
13	1.4	200	3.87	1.21	90.67	22.59
14	1.4	220	4.30	1.22	90.66	23.61
15	1.4	240	4.74	1.23	90.66	24.51
16	1.5	160	3.13	1.19	90.51	20.94
17	1.5	180	3.57	1.17	90.64	22.25
18	1.5	200	4.03	1.16	90.29	23.43
19	1.5	220	4.48	1.17	90.21	24.46
20	1.5	240	4.93	1.18	90.22	25.42

Table S3. Simulation results of different feed flow rates and Cv at 4000 m.

No.	Cv mol/s/MPa	Feed Flowrate m^3/h	Pro. m^3/h	En. MJ/m^3	Pur. %	Rec. %
1	1.2	160	2.34	1.39	91.57	17.89
2	1.2	180	2.68	1.37	91.52	19.06
3	1.2	200	3.01	1.37	91.53	20.08
4	1.2	220	3.35	1.37	91.54	20.99
5	1.2	240	3.69	1.38	91.55	21.80
6	1.3	160	2.46	1.32	91.26	18.73
7	1.3	180	2.81	1.30	91.16	19.96
8	1.3	200	3.17	1.29	91.15	21.02
9	1.3	220	3.52	1.30	91.13	21.98
10	1.3	240	3.87	1.31	91.19	22.83
11	1.4	160	2.57	1.26	90.94	19.50
12	1.4	180	2.94	1.24	90.80	20.79
13	1.4	200	3.31	1.23	90.74	21.89
14	1.4	220	3.68	1.23	90.74	22.89
15	1.4	240	4.05	1.25	90.75	23.78
16	1.5	160	2.67	1.20	90.60	20.22
17	1.5	180	3.06	1.18	90.41	21.56
18	1.5	200	3.45	1.18	90.33	22.70
19	1.5	220	3.83	1.18	90.24	23.72
20	1.5	240	4.22	1.19	90.28	24.65

Table S4. Simulation results of different feed flow rate and Cv at 5000 m.

No.	Cv mol/s/MPa	Feed Flowrate m^3/h	Pro. m^3/h	En. MJ/m^3	Pur. %	Rec. %
1	1.2	160	2.00	1.41	91.55	17.34
2	1.2	180	2.28	1.39	91.52	18.48
3	1.2	200	2.57	1.38	91.53	19.49
4	1.2	220	2.85	1.39	91.55	20.38
5	1.2	240	3.14	1.40	91.57	21.17
6	1.3	160	2.10	1.33	91.23	18.17
7	1.3	180	2.39	1.31	91.19	19.34
8	1.3	200	2.70	1.31	91.16	20.40
9	1.3	220	3.00	1.31	91.16	21.33
10	1.3	240	3.30	1.33	91.19	22.17
11	1.4	160	2.19	1.27	90.89	18.96
12	1.4	180	2.50	1.25	90.83	20.13
13	1.4	200	2.82	1.24	90.77	21.25
14	1.4	220	3.13	1.25	90.75	22.21

15	1.4	240	3.45	1.26	90.74	23.08
16	1.5	160	2.29	1.21	90.52	19.68
17	1.5	180	2.60	1.19	90.46	20.86
18	1.5	200	2.93	1.19	90.35	22.03
19	1.5	220	3.26	1.19	90.31	23.02
20	1.5	240	3.59	1.20	90.30	23.92